Comparison of UV-A photolytic and UV/TiO2 photocatalytic effects on Microcystis aeruginosa PCC7813 and four microcystin analogues: a pilot scale study. [Dataset]

MENEZES, I., CAPELO-NETO, J., PESTANA, C.J., CLEMENTE, A., HUI, J., IRVINE, J.T.S., GUNARATNE, H.Q.N., ROBERTSON, P.K.J., EDWARDS, C., GILLANDERS, R.N., TURNBULL, G.A. and LAWTON, L.A.

2021

Supplementary information

Comparison of UV photolytic and UV/TiO_2 photocatalytic effects on *Microcystis aeruginosa* PCC7813 and four microcystin analogues: a pilot scale study

Indira Menezes[a,b*], José Capelo-Neto[a], Carlos J. Pestana[b], Allan Clemente[a], Jianing Hui[c], John T. S. Irvine[c], H.Q. Nimal Gunaratne[d], Peter K.J. Robertson[d], Christine Edwards[b], Ross N. Gillanders[e], Graham A. Turnbull[e], Linda A. Lawton[b]

[a] Department of Hydraulic and Environmental Engineering, Federal University of Ceará, Fortaleza, Brazil

[b] School of Pharmacy and Life Sciences, Robert Gordon University, Aberdeen, United Kingdom

[c] School of Chemistry, University of St Andrews, St Andrews, United Kingdom

[d] School of Chemistry and Chemical Engineering, Queen's University, Belfast, United Kingdom

[e] Organic Semiconductor Centre, SUPA, School of Physics and Astronomy, University of St Andrews, St Andrews, United Kingdom

*Corresponding author: i.de-menezes-castro@rgu.ac.uk

Number of tables: 2

Number of figures: 32

S1 Reactor system

Reactors were placed inside acrylic cylinders (1100 x 95 mm) containing 6.5 liters of *M. aeruginosa* PCC7813 suspension (Figure S1) and sparged with sterile air from the bottom. Triplicate reactors were used for each tested system: UV-only containing UV-A LED strips and empty tetrahedral pods (Figure S1A), TiO_2-only containing TiO_2 coated beads inside tetrahedral pods (Figure S1B) and UV/TiO_2 containing TiO_2 coated beads in tetrahedral pods illuminated by UV-A LED strips (Figure S1C).

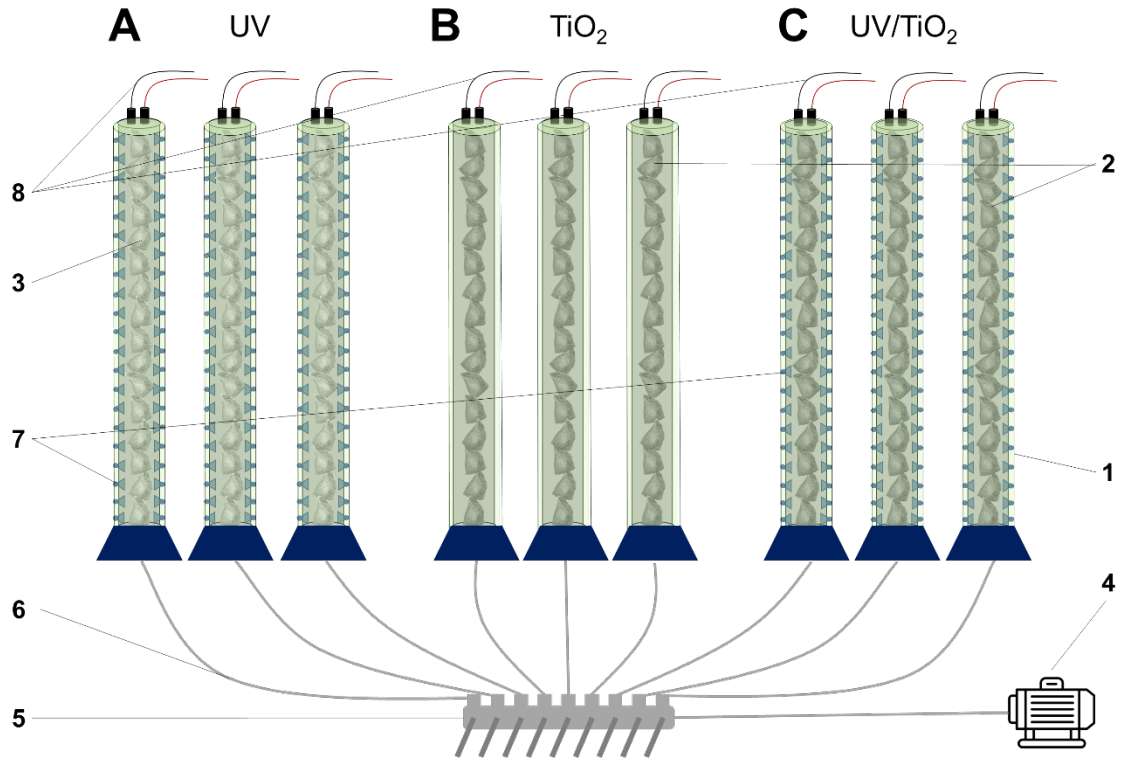

Figure S1 – Schematic representation of the experimental reactors design for (A) UV photolysis, (B) TiO_2-only and (C) UV/TiO_2 photocatalysis. 1 – acrylic cylinders containing the stainless-steel reactors, 2 – stainless-steel pods containing TiO_2 coated beads, 3 – empty stainless-steel pods, 4 – aeration pump for continuous gentle air flow, 5 – air flow distributor to achieve equal air pressure across all samples, 6 – silicone tubes connecting the air flow distribution and the reactors, 7 – UV light from UV-LED strip, 8 – power source connection.

Titanium dioxide porous glass beads were placed inside of tetrahedral pods manufactured from a stainless-steel mesh with aperture of 1.2 x 1.2 mm and wire strength of 0.4 mm. Stainless-steel sheets were cut (15 x 13 cm) and then folded into the final tetrahedral form of pods (Figure S2). Empty pods were also used during UV

photolysis evaluation.

Figure S2 – Stainless-steal tetrahedral pod containing TiO_2 coated porous recycled glass beads used during *Microcystis aeruginosa* PCC7813 and microcystins photocatalytic treatment under UV/LED irradiation containing titanium dioxide coated porous glass beads.

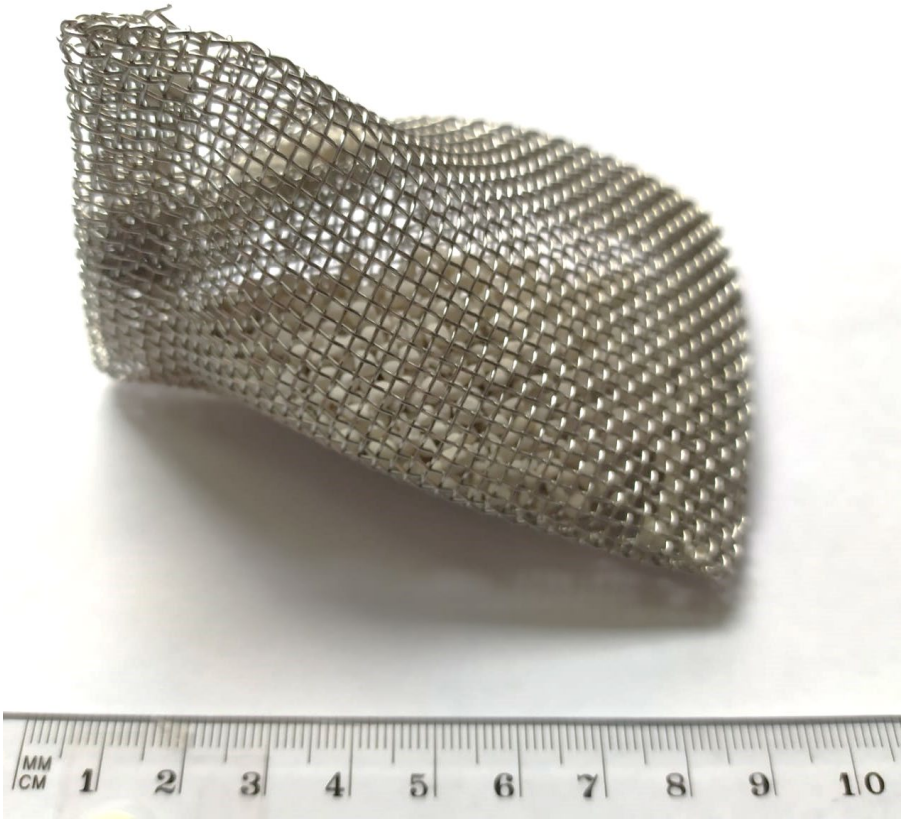

S2 Temperature monitoring

Temperature of the solution was measured (Table S1) for each reactor (UV-only, TiO_2-only and UV/TiO_2) just after sampling had occurred using a digital thermometer (Fisher Scientific, UK). The average temperature for UV-only, TiO_2-only and UV/TiO_2 was 22.1 ± 0.1, 21.1 ± 0.1 and 22.1± 0.2 °C respectively, therefore, no marked temperature variation was observed for those reactors containing UV irradiation.

Table S1 – Temperature (°C) measurements for each individual reactor of UV-only, TiO_2-only and UV/TiO_2 throughout 14 days of experiment right after sampling have occurred.

Sampling time (days)	Temperature (°C)								
	UV			TiO_2			UV/TiO_2		
0	20.8	20.8	20.8	20.9	21.1	21.0	20.9	20.7	21.0
1	21.5	21.5	21.5	20.4	20.6	20.7	21.7	21.6	21.3
2	21.5	21.6	21.4	20.6	20.5	20.4	21.7	21.6	21.4
3	22.0	21.8	21.8	21.0	20.7	20.5	22.2	21.6	22.0
4	21.7	21.6	21.5	20.5	20.3	20.5	22.5	21.7	21.7
5	22.2	21.8	22.3	21.5	21.4	21.4	21.9	21.6	21.6
6	23.6	24.1	23.8	22.6	22.6	22.4	23.4	24.1	23.8
7	23.0	23.1	22.8	22.0	21.7	21.7	22.2	22.0	22.0
8	23.0	22.7	22.8	21.7	21.7	21.7	23.1	22.9	22.5
9	22.3	22.3	22.5	21.7	21.5	21.4	22.1	22.2	22.3
10	21.5	21.6	21.7	20.9	20.8	20.6	21.6	21.7	21.8
11	21.1	20.9	20.7	20.1	20.0	19.9	21.2	21.3	21.1
12	21.8	22.1	22.1	20.9	21.0	21.2	22.5	22.3	21.9
13	22.5	22.5	22.5	21.3	21.1	21.2	22.2	22.2	22.5
14	23.1	23.6	22.9	21.9	21.8	21.6	23.1	23.4	22.7

S3 *Microcystis aeruginosa* PCC7813 regrowth experimental design

Microcystis aeruginosa PCC7813 cellular regrowth was evaluated (Figure S3) over 7 days to evaluate potential cyanobacterial recovery under optimal conditions after different treatments. After the treatments, aliquots containing *Microcystis aeruginosa* PCC7813 (1.5 mL) were added to BG-11 medium (1.5 mL) inside four 4 mL glass vials that were placed in a 150 mL beaker.

Figure S3 – (A) Top view and (B) side view representation of 150 mL beaker and 4 mL vials used in the *Microcystis aeruginosa* PCC7813 regrowth experiment stored at 21±1 °C on a 12/12 hours light/dark cycle illuminated by cool white fluorescent lights with an average light intensity of 10.5 µmol photons m^{-2} s^{-1} without agitation

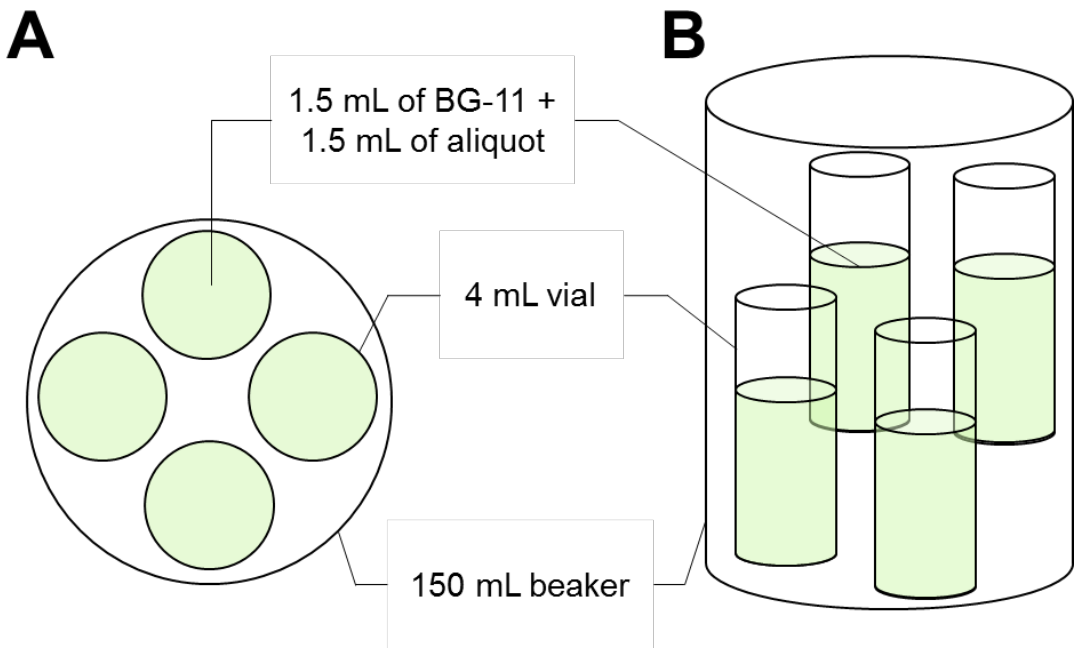

S4 Statistical data analysis

The type of statistical model (linear, piecewise, linear-plateau, exponential and logarithmic regression) was selected for each dependent variable for each type of treatment according to the values of R^2, adjusted R^2, Akaike information criteria (AIC) and Bayesian information criteria (BIC). The models that presented the highest R^2 and adjusted R^2 and the lowest AIC and BIC were chosen (Table S2).

The graphic data analysis for each type of treatment (i.e., UV/TiO_2, TiO_2-only and UV) showed that the results can be interpreted using two classes of statistical models: linear, which shows a linear relation between dependent and independent variables, (Equation S1) and piecewise regression, which consists in multiple linear models for different ranges of the independent variable (Equation S2).

$$Y = \beta_0 + \beta_1 X \qquad \text{Equation S1}$$

$$Y = \begin{cases} \beta_0 + \beta_1 X, & X \leq \theta \\ \beta_0 + \beta_2 X + \theta(\beta_1 - \beta_2), & X > \theta \end{cases} \qquad \text{Equation S2}$$

Where Y is the dependent variable (cell density during the treatment and intra- and extracellular microcystins), β_0 is the intercept, β_1 and β_2 are the coefficients of the

independent variable of each model, X is the independent variable (time) and θ is the breakpoint that determines the change in the behavior of the dependent variables for the piecewise regression model. The breakpoint is also where the inclination of the linear function changes. Each dependent variable demonstrated a different breakpoint θ.

Each model was considered adjusted when the requirements simultaneously fit:

- Independent variable (day) coefficients significant (p<0.05) by t-test.
- Obtained model shows significant F-statistics (p<0.05).
- Confidence interval of independent variable (day) coefficients estimated by 95% do not contain the value 0.
- Graphic analysis of residues, i.e., residuals vs fitted (homoscedasticity) and Q-Q plot – normality (Figure S4 – S30). For the graphic analysis of homoscedasticity and residuals vs leverage, all the points must be randomly distributed around 0, while the Q-Q plot – normality graph must show all the points distributed around a straight line and the scale-location.

Table S2 – Values of R^2, adjusted R^2, Akaike information criteria (AIC) and Bayesian information criteria (BIC) for selection of model (linear or piecewise regression) for the dependent variable cell density during UV/TiO_2 treatment.

Treatment	Analysis	R^2	Adjusted R^2	AIC	BIC	Model chosen
UV	Cell density	0.97	0.97	15.41	18.25	Piecewise regression
TiO_2	Cell density	0.73	0.71	28.01	30.14	Linear regression
UV/TiO_2	Cell density	0.79	0.75	33.41	36.24	Piecewise regression
UV	Intracellular MC-LR	0.97	0.96	-84.67	-81.84	Piecewise regression
TiO_2	Intracellular MC-LR	0.46	0.42	-72.92	-70.79	Linear regression
UV/TiO_2	Intracellular MC-LR	0.34	0.23	-54.92	-52.09	Piecewise regression
UV	Intracellular MC-LY	0.97	0.96	-166.83	-164	Piecewise regression
TiO_2	Intracellular MC-LY	0.72	0.7	-161.41	-159.29	Linear regression

UV/TiO_2	Intracellular MC-LY	0.54	0.46	-142.69	-139.86	Piecewise regression
UV	Intracellular MC-LW	0.97	0.96	-113.53	-110.7	Piecewise regression
TiO_2	Intracellular MC-LW	0.86	0.85	-110.23	-108.1	Linear regression
UV/TiO_2	Intracellular MC-LW	0.58	0.51	-90.07	-87.24	Piecewise regression
UV	Intracellular MC-LF	0.97	0.96	-102.99	-100.16	Piecewise regression
TiO_2	Intracellular MC-LF	0.77	0.76	-102.62	-100.5	Linear regression
UV/TiO_2	Intracellular MC-LF	0.62	0.56	-81.07	-78.24	Linear regression
UV	Extracellular MC-LR	0.72	0.68	-113	-110.17	Piecewise regression
TiO_2	Extracellular MC-LR	0.11	0.04	-117.25	-115.13	Linear regression
UV/TiO_2	Extracellular MC-LR	0.57	0.54	-116.74	-114.62	Linear regression
UV	Extracellular MC-LY	0.74	0.69	-196.05	-193.21	Piecewise regression
TiO_2	Extracellular MC-LY	0.04	-0.04	-203.01	-200.88	Linear regression
UV/TiO_2	Extracellular MC-LY	0.37	0..06	-0.01	-214.37	Linear regression
UV	Extracellular MC-LW	0.44	0.34	-130.17	-127.34	Piecewise regression
TiO_2	Extracellular MC-LW	0.11	0.04	-138.57	-136.45	Linear regression
UV/TiO_2	Extracellular MC-LW	0.03	-0.04	-153.27	-151.15	Linear regression
UV	Extracellular MC-LF	0.70	0.66	-125.67	-122.84	Piecewise regression
TiO_2	Extracellular MC-LF	0.07	0	-131.08	-128.96	Linear regression
UV/TiO_2	Extracellular MC-LF	0.37	0.33	-136.83	-134.7	Linear regression

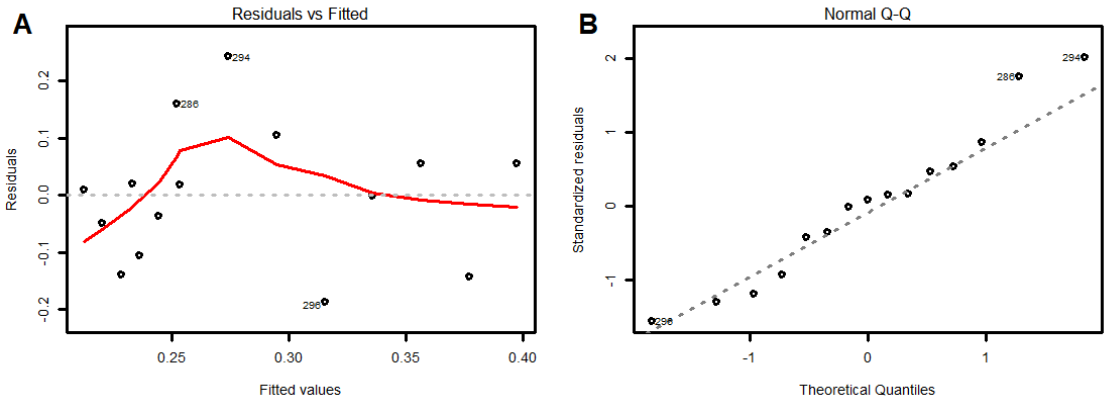

Figure S4 – Graphic analysis of residuals according to criteria A) homoscedasticity and B) Q-Q plot – normality for the dependent variable cell density during UV treatment.

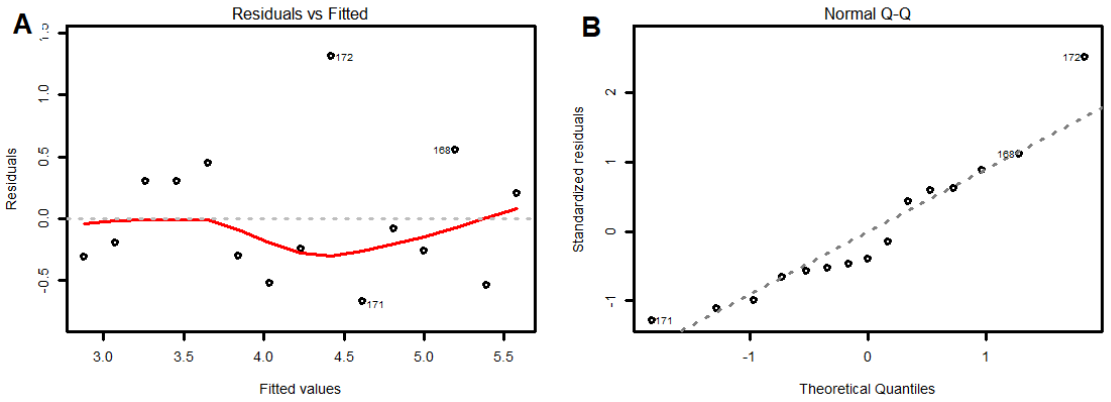

Figure S5 – Graphic analysis of residuals according to criteria A) homoscedasticity and B) -Q plot – normality for the dependent variable cell density during TiO_2 treatment.

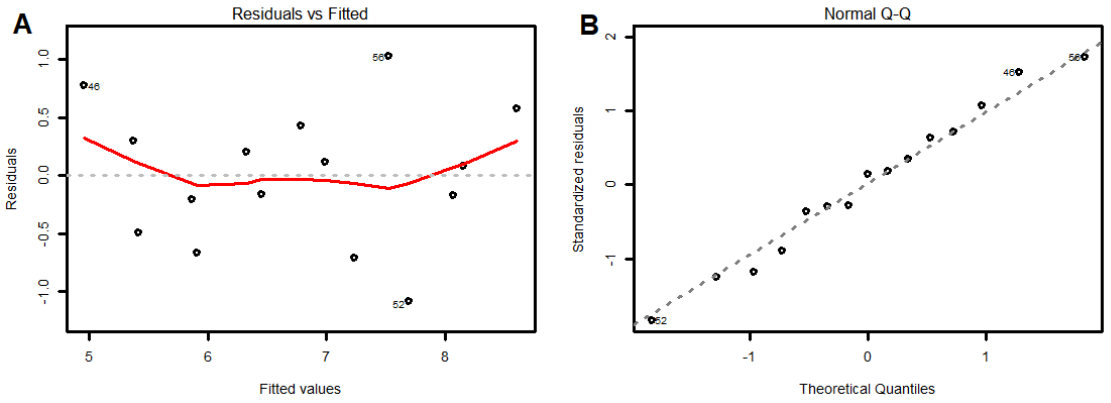

Figure S6 – Graphic analysis of residuals according to criteria A) homoscedasticity and B) Q-Q plot – normality for the dependent variable cell density during UV/TiO_2 treatment.

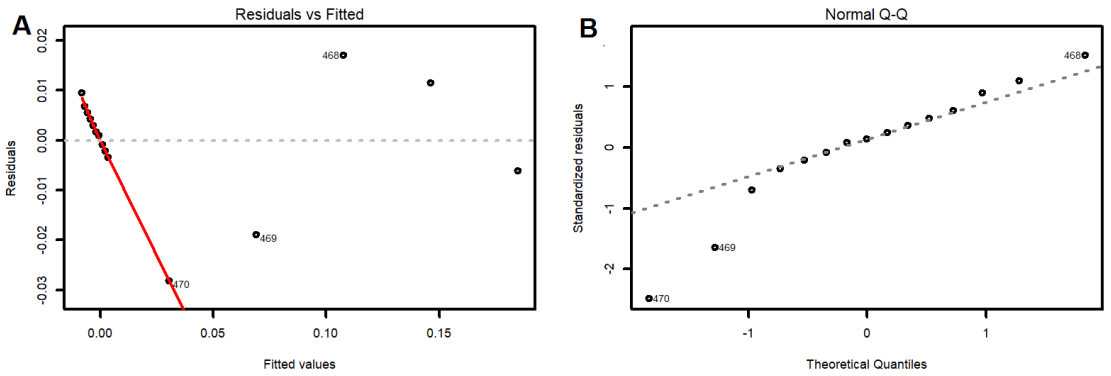

Figure S7 – Graphic analysis of residuals according to criteria A) homoscedasticity and B) Q-Q plot – normality for the dependent variable intracellular microcystin-LR during UV treatment.

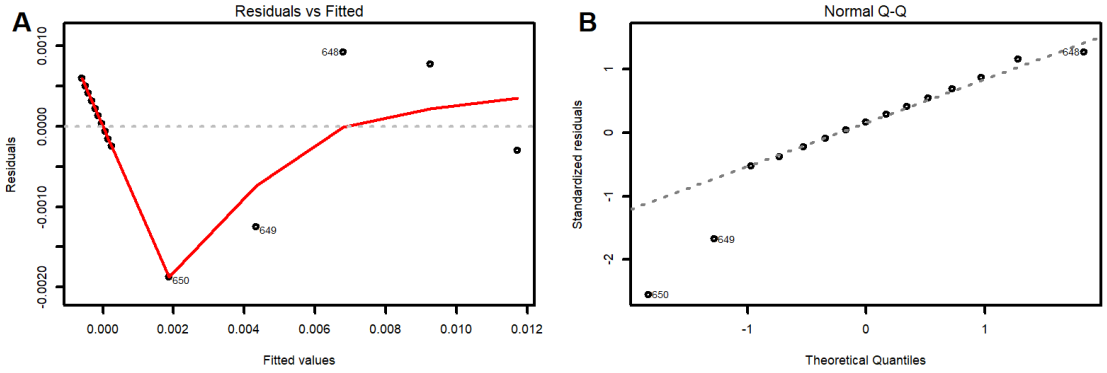

Figure S8 – Graphic analysis of residuals according to criteria A) homoscedasticity and B) Q-Q plot – normality for the dependent variable intracellular microcystin-LY during UV treatment.

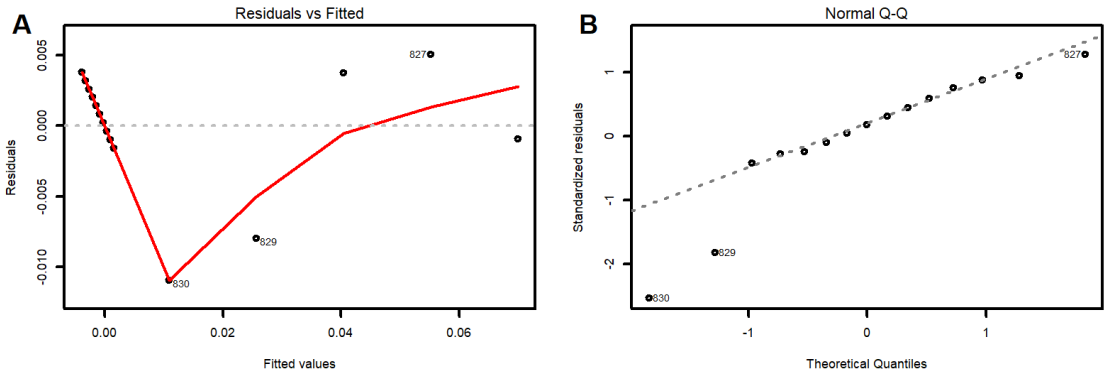

Figure S9 – Graphic analysis of residuals according to criteria A) homoscedasticity and B) Q-Q plot – normality for the dependent variable intracellular microcystin-LW during UV treatment.

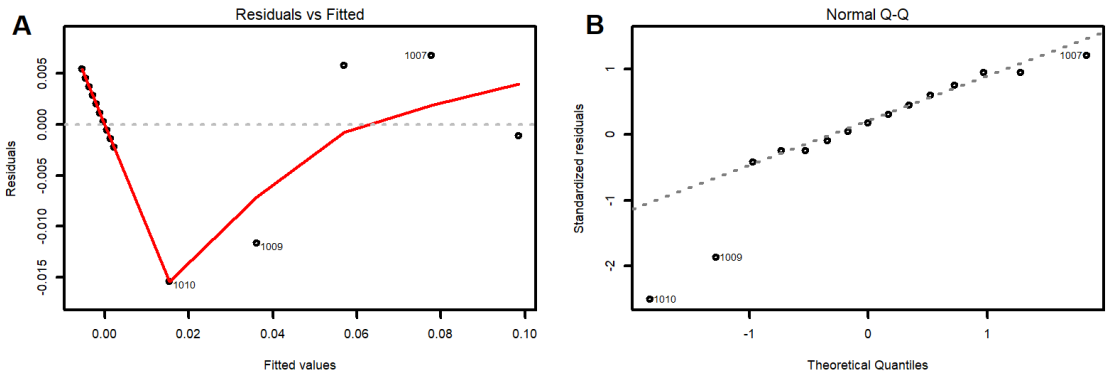

Figure S10 – Graphic analysis of residuals according to criteria A) homoscedasticity and B) Q-Q plot – normality for the dependent variable intracellular microcystin-LF during UV treatment.

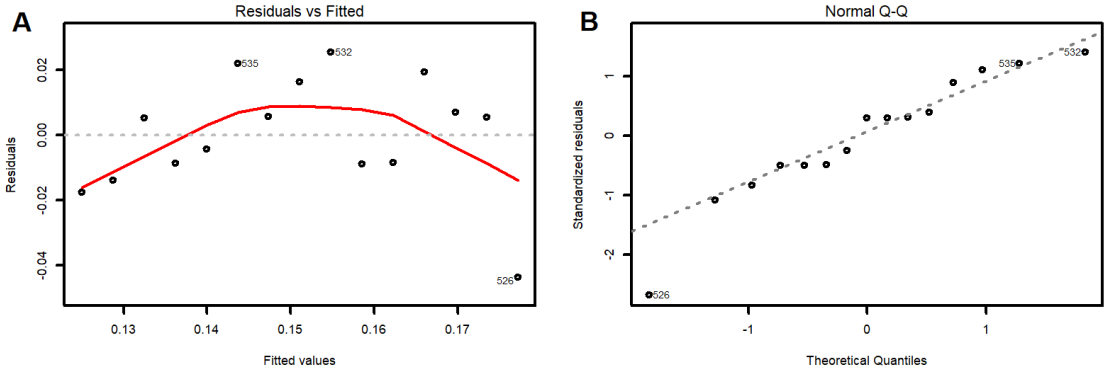

Figure S11 – Graphic analysis of residuals according to criteria A) homoscedasticity and B) Q-Q plot – normality for the dependent variable intracellular microcystin-LR during TiO_2 treatment.

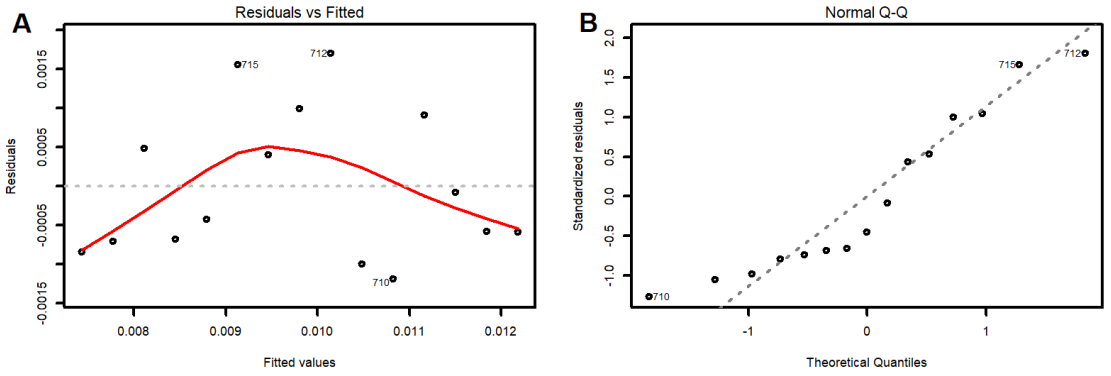

Figure S12 – Graphic analysis of residuals according to criteria A) homoscedasticity and B) Q-Q plot – normality for the dependent variable intracellular microcystin-LY during TiO_2 treatment.

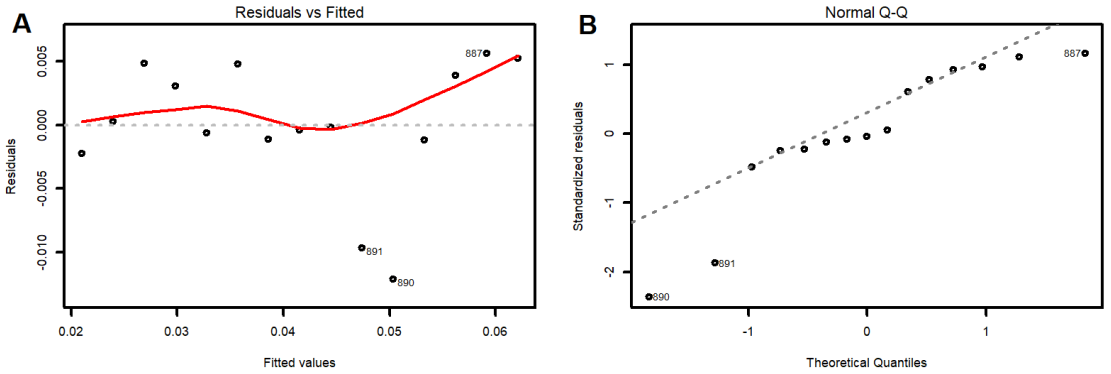

Figure S13 – Graphic analysis of residuals according to criteria A) homoscedasticity and B) Q-Q plot – normality for the dependent variable intracellular microcystin-LW during TiO_2 treatment.

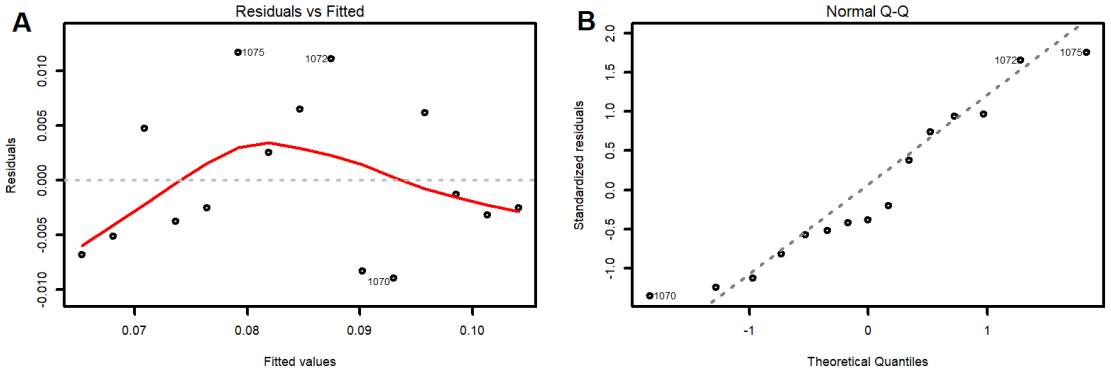

Figure S14 – Graphic analysis of residuals according to criteria A) homoscedasticity and B) Q-Q plot – normality for the dependent variable intracellular microcystin-LF during TiO_2 treatment.

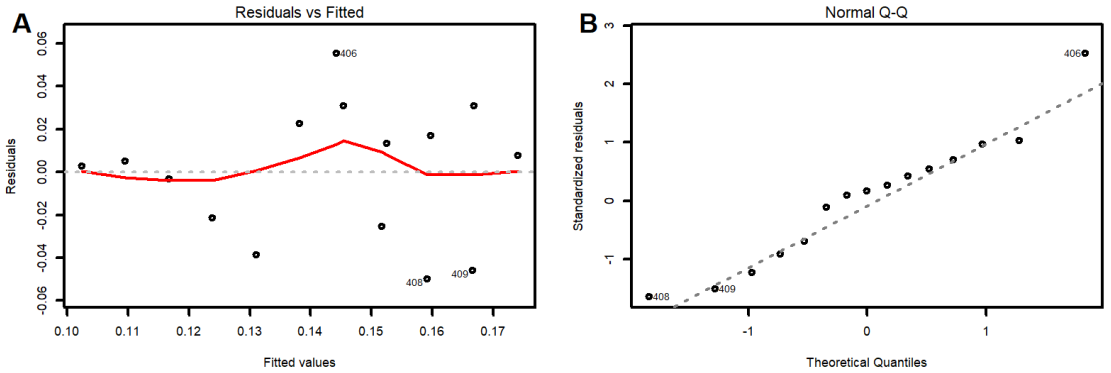

Figure S15 – Graphic analysis of residuals according to criteria A) homoscedasticity and B) Q-Q plot – normality for the dependent variable intracellular microcystin-LR during UV/TiO_2 treatment

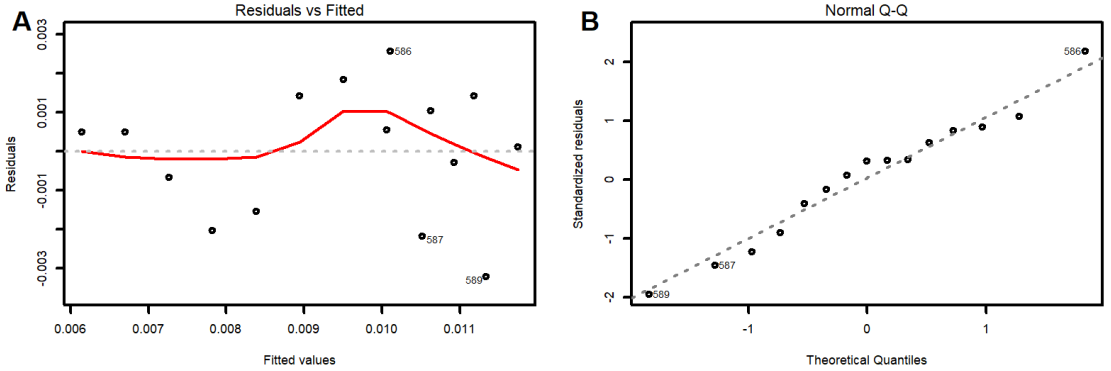

Figure S16 – Graphic analysis of residuals according to criteria A) homoscedasticity and B) Q-Q plot – normality for the dependent variable intracellular microcystin-LY during UV/TiO_2 treatment.

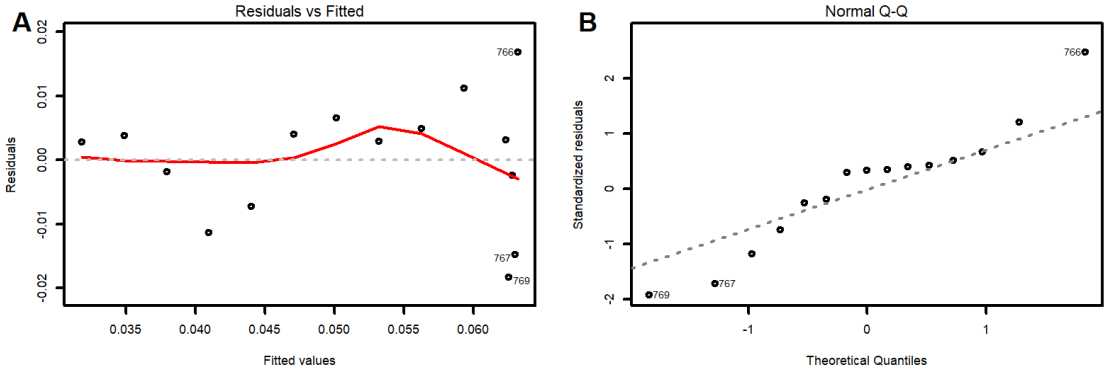

Figure S17 – Graphic analysis of residuals according to criteria A) homoscedasticity and B) Q-Q plot – normality for the dependent variable intracellular microcystin-LW during UV/TiO_2 treatment.

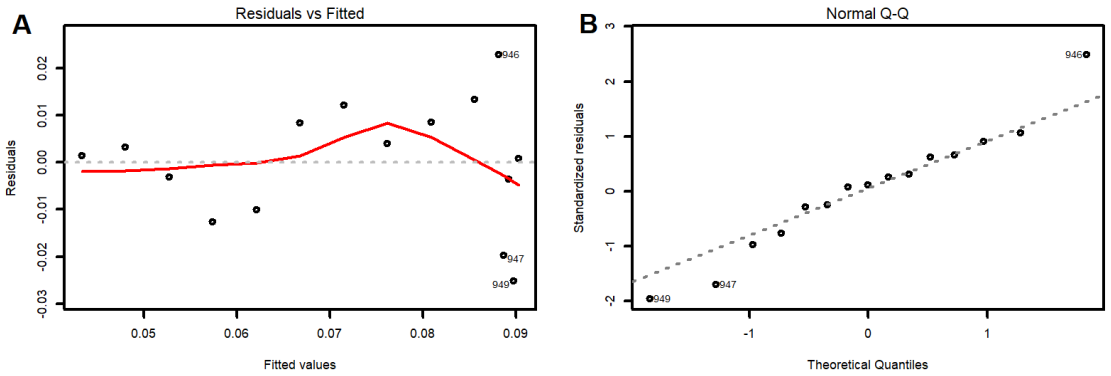

Figure S18 – Graphic analysis of residuals according to criteria A) homoscedasticity and B) Q-Q plot – normality for the dependent variable intracellular microcystin-LF during UV/TiO_2 treatment.

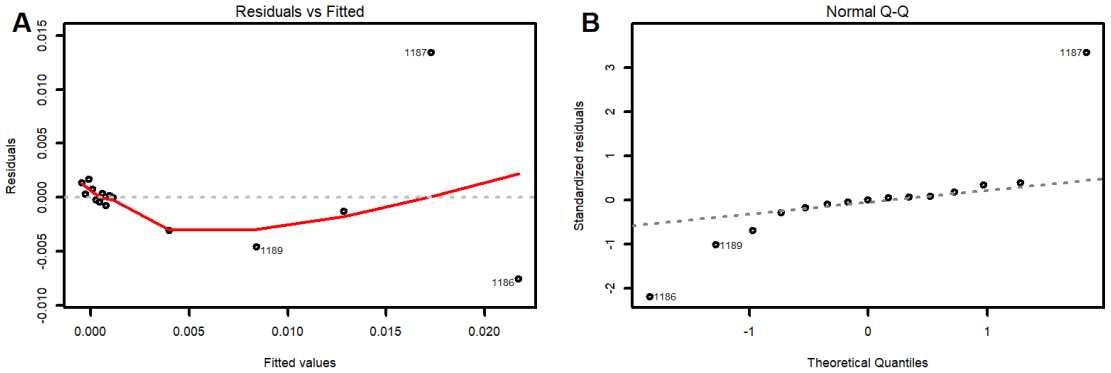

Figure S19 – Graphic analysis of residuals according to criteria A) homoscedasticity and B) Q-Q plot – normality for the dependent variable extracellular microcystin-LR during UV treatment.

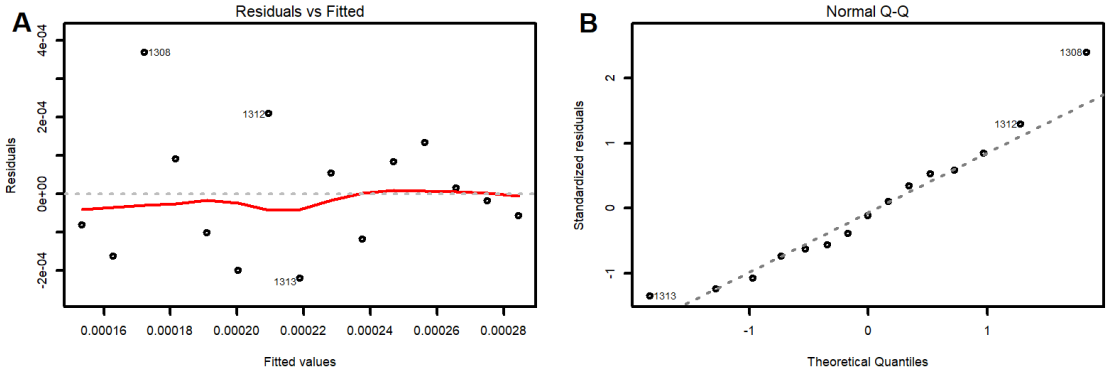

Figure S20 – Graphic analysis of residuals according to criteria A) homoscedasticity and B) Q-Q plot – normality for the dependent variable extracellular microcystin-LY during UV treatment.

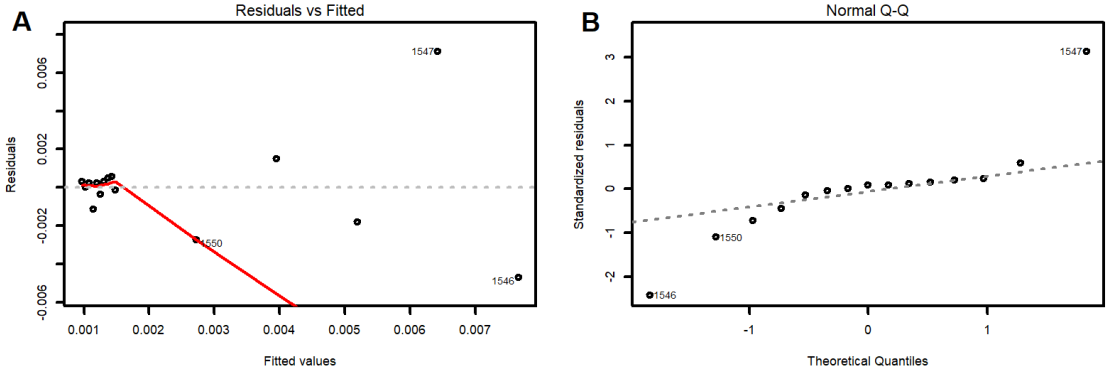

Figure S21 – Graphic analysis of residuals according to criteria A) homoscedasticity and B) Q-Q plot – normality for the dependent variable extracellular microcystin-LW during UV treatment.

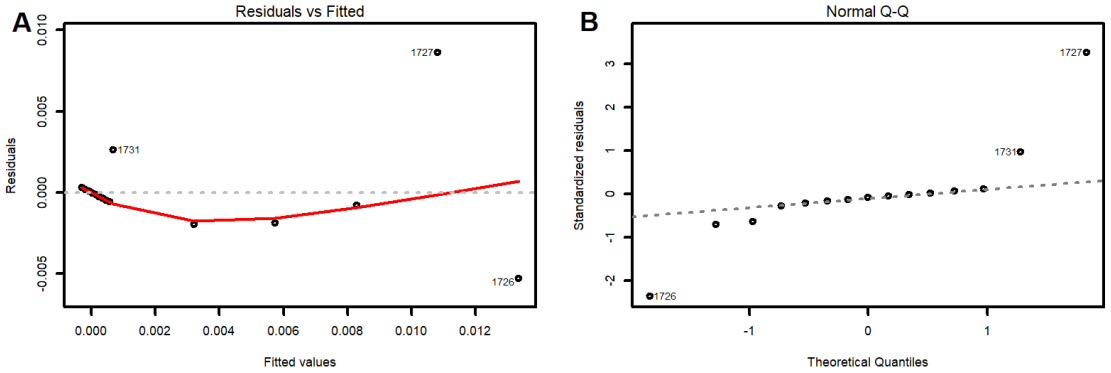

Figure S22 – Graphic analysis of residuals according to criteria A) homoscedasticity B) Q-Q plot – normality for the dependent variable extracellular microcystin-LF during UV treatment.

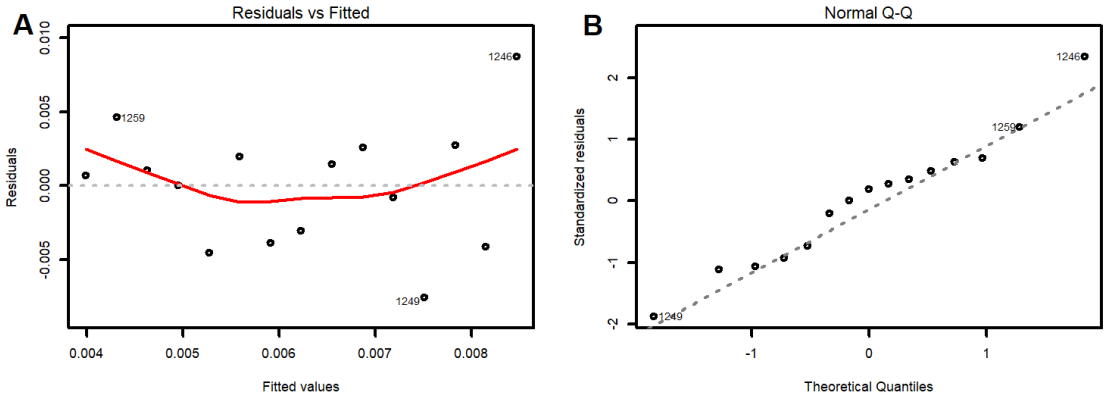

Figure S23 – Graphic analysis of residuals according to criteria A) homoscedasticity and B) Q-Q plot – normality for the dependent variable extracellular microcystin-LR during TiO_2 treatment.

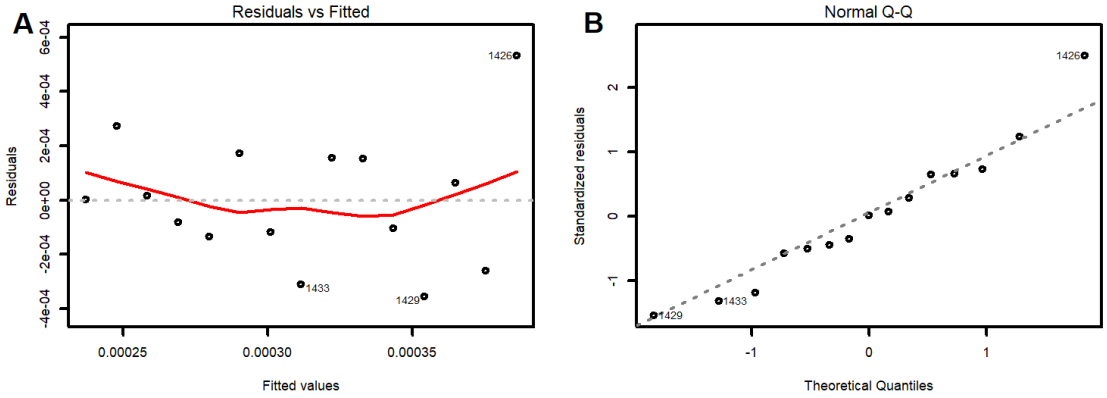

Figure S24 – Graphic analysis of residuals according to criteria A) homoscedasticity and B) Q-Q plot – normality for the dependent variable extracellular microcystin-LY during TiO_2 treatment.

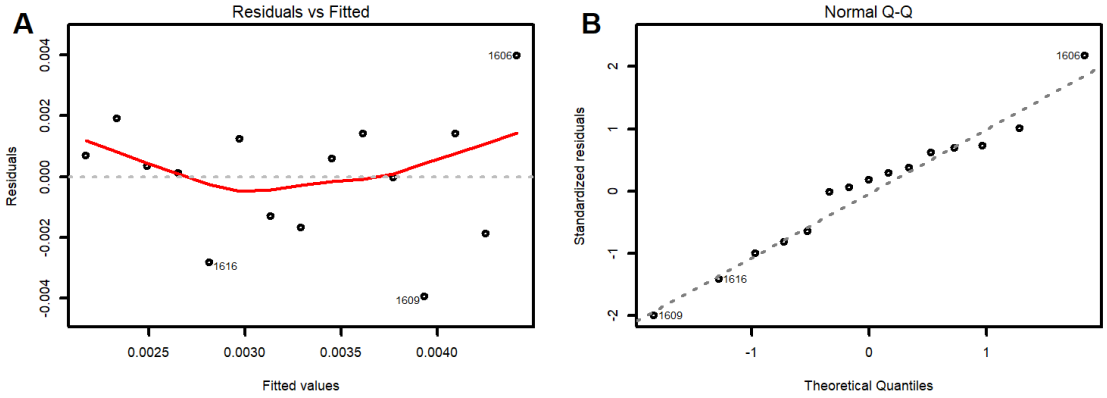

Figure S25 – Graphic analysis of residuals according to criteria A) homoscedasticity and B) Q-Q plot – normality for the dependent variable extracellular microcystin-LW during TiO_2 treatment.

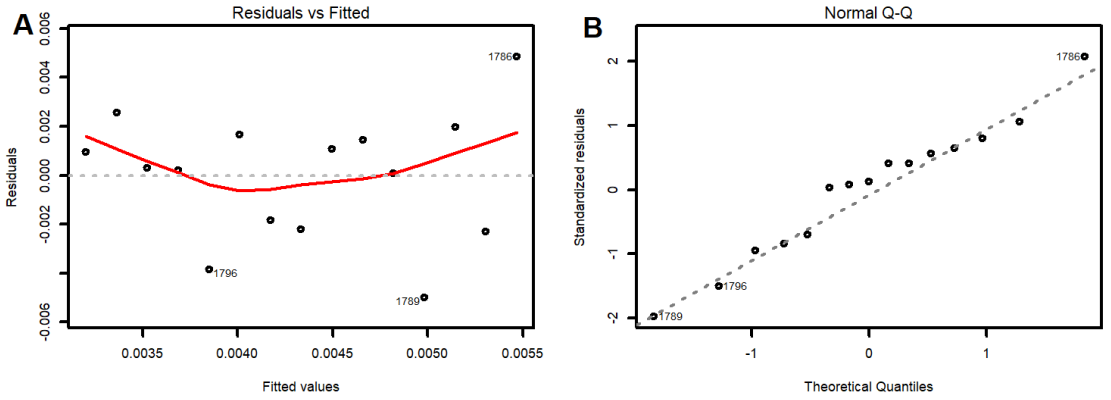

Figure S26 – Graphic analysis of residuals according to criteria A) homoscedasticity and B) Q-Q plot – normality for the dependent variable extracellular microcystin-LF during TiO_2 treatment.

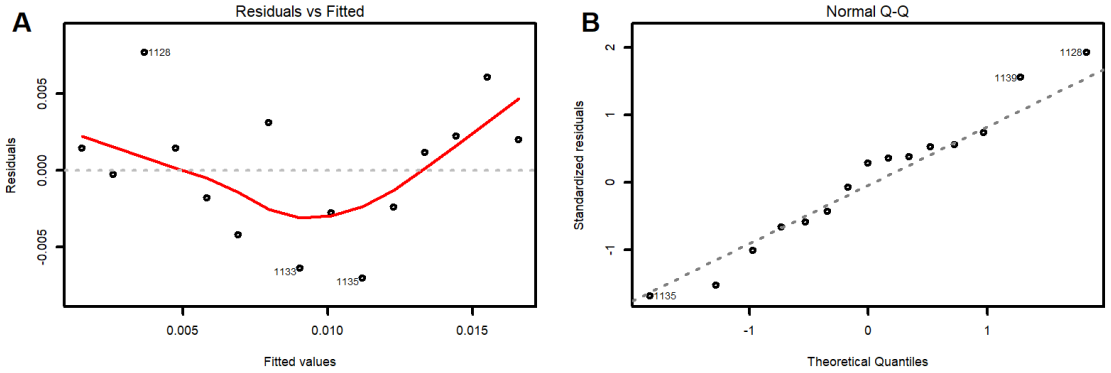

Figure S27 – Graphic analysis of residuals according to criteria A) homoscedasticity and B) Q-Q plot – normality for the dependent variable extracellular microcystin-LR during UV/TiO_2 treatment.

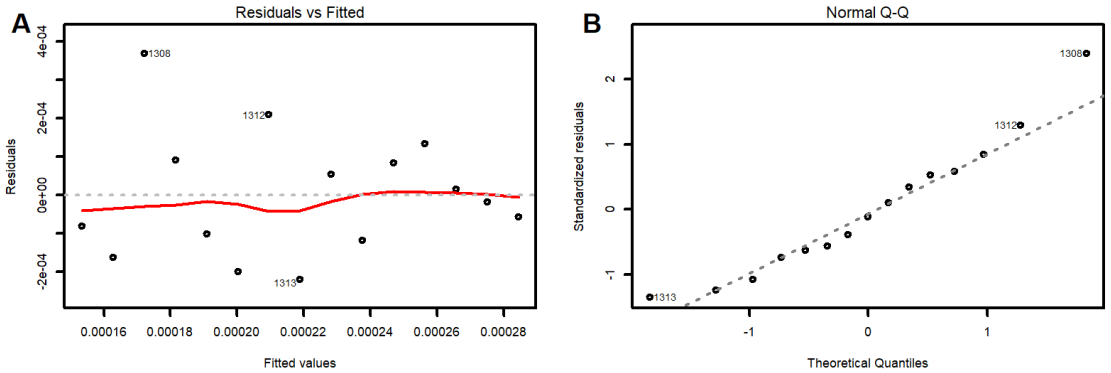

Figure S28 – Graphic analysis of residuals according to criteria A) homoscedasticity and B) Q-Q plot – normality for the dependent variable extracellular microcystin-LY during UV/TiO_2 treatment.

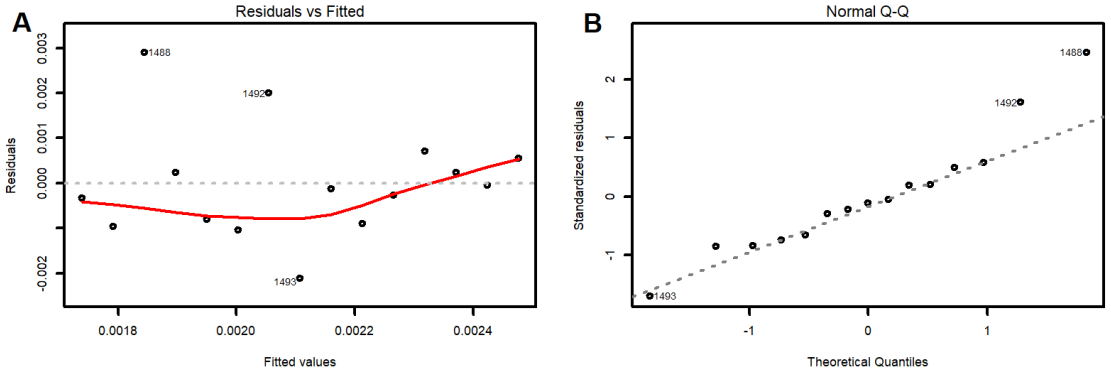

Figure S29 – Graphic analysis of residuals according to criteria A) homoscedasticity and B) Q-Q plot – normality for the dependent variable extracellular microcystin-LW during UV/TiO_2 treatment.

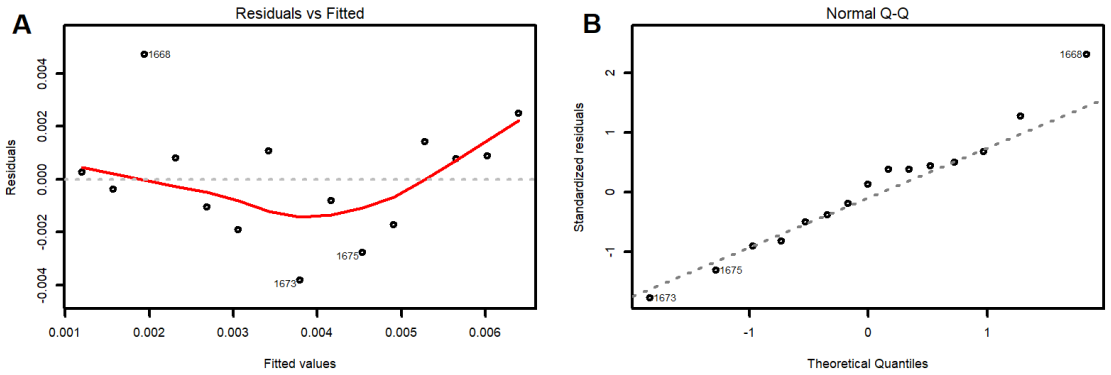

Figure S30 – Graphic analysis of residuals according to criteria A) homoscedasticity and B) Q-Q plot – normality for the dependent variable extracellular microcystin-LF during UV/TiO_2 treatment.

S5 Photoluminescence measurements of TiO_2 coated glass beads

Photoluminescence measurements of both uncoated and TiO_2 coated beads were performed to verify if any UV illumination was converted into visible light during treatment. For the photoluminescence quantum yield (PLQY) under 365 nm illumination, the beads were loaded into a UV-transparent cuvette in air and the absolute photoluminescence quantum efficiency was measured using Hamamastu PLQY instrument.

Both uncoated and TiO_2 coated beads presented deep-blue photoluminescence (Figure S31), with a low quantum efficiency of 4% (uncoated sample) and 7% (TiO_2 coated sample). The data showed that the beads do generate additional visible light,

albeit with low efficiency. The spectrum had good overlap with the blue absorption peak of chlorophyll *a* (Figure S32), and so may contributed to growth of the cyanobacteria.

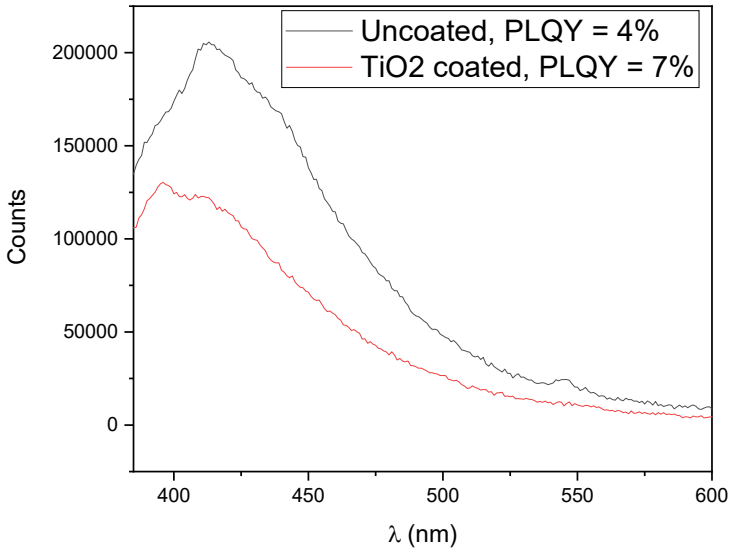

Figure S31 – Fluorescence spectra of uncoated glass beads (black line) and TiO_2 coated glass beads (red line) with an excitation wavelength of 365 nm.

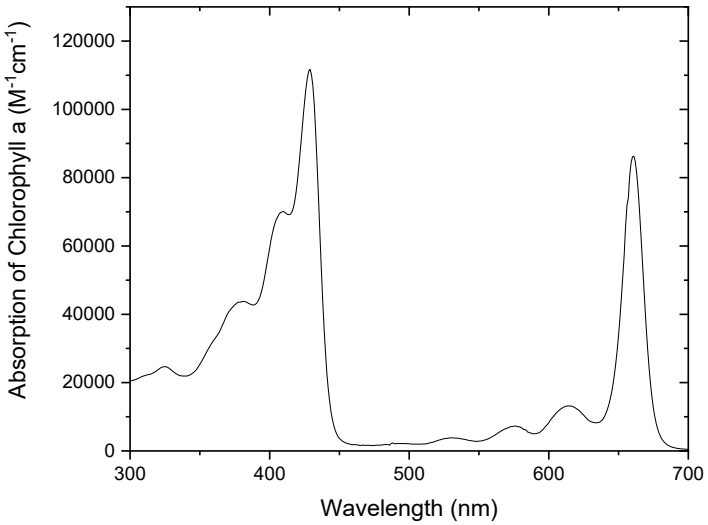

Figure S32 – Absorption spectrum of chlorophyll *a*. Data from PhotochemCAD database: Taniguchi (2018).

S6 Reference

Taniguchi, M.; Lindsey, J. S., 2018. Database of Absorption and Fluorescence Spectra of >300 Common Compounds for Use in PhotochemCAD, Photochem. Photobiol. 94, 290–327. https://doi.org/10.1111/php.12860.